

## The Effect of Ru Substitution on the Electrical and Humidity Sensor Properties of Semiconductor Tin Oxide Film

Ömer MERMER<sup>1,2</sup>, Mustafa EROL<sup>2,3,4</sup>, Murat BEKTAŞ<sup>2</sup> ve Erdal ÇELİK<sup>2,3,5</sup>

<sup>1</sup>Ege University, Engineering Faculty, Department of Electrical and Electronics Engineering, Bornova, İzmir, Turkey

<sup>2</sup>Dokuz Eylül University, Center for Fabrication and Application of Electronic Materials, Buca, İzmir, Turkey

<sup>3</sup>Dokuz Eylül University, Department of Metallurgical and Materials Engineering, Buca, İzmir, Turkey

<sup>4</sup>Dokuz Eylül University, Graduate School Natural and Applied Sciences, Metallurgical and Materials Engineering, Buca, İzmir, Turkey

<sup>5</sup>Dokuz Eylül University, Graduate School Natural and Applied Sciences, Nanoscience and Nanoengineering, Buca, İzmir, Turkey

e-posta: omermermer@gmail.com

Geliş Tarihi: 26.10.2012; Kabul Tarihi: 11.11.2013

### Abstract

In this study, pure SnO<sub>2</sub> and Ru-SnO<sub>2</sub> thin films were deposited on Si and glass substrates via sol-gel technique for humidity sensor applications. Transparent solutions were prepared from Sn and Ru based precursors. The solutions were deposited on Si (100) and glass substrates by using spin coating technique which provides thin and smooth films. The thin films were annealed at 600°C for 1 hour in air to obtain SnO<sub>2</sub> based films. The structural and electrical properties of the films were characterized by XRD, SEM, source/meter system respectively. The AC and DC electrical conductivity of the pure and Ru-doped SnO<sub>2</sub> films were determined. Humidity sensing properties were measured changing the electrical resistance for different humidity levels at room temperature. The humidity adsorption kinetics of these films was investigated by quartz crystal microbalance (QCM) technique.

### Key words

Ru doping; Tin oxide;  
Sol-gel; Humidity  
sensor

## Ru Katkısının Yarıiletken Kalay Oksit Filmlerin Elektriksel ve Nem Sensörü Özelliklerine Etkisi

### Özet

Bu çalışmada nem sensörü uygulaması için saf ve Ru katkılı SnO<sub>2</sub> ince filmler Si ve cam altlıklar üzerine sol-jel yöntemi kullanılarak kaplanmıştır. Kalay ve rutenyum tabanlı prekursorlar kullanılarak şeffaf çözeltiler hazırlanmıştır. Bu çözeltilerle Si (100) ve cam altlıklar üzerine döndürerek kaplama tekniği kullanılarak ince ve homojen dağılımlı filmler kaplanmıştır. Elde edilen filmler 600°C'de 1 saat fırınlandıktan sonra SnO<sub>2</sub> tabanlı filmler elde edilmiştir. Üretilen filmlerin yapısal ve elektriksel karakterizasyonu sırasıyla XRD, SEM, kaynak-metre sistemleri kullanılarak yapılmıştır. Saf ve Ru katkılı SnO<sub>2</sub> ince filmlerin AC ve DC elektriksel iletkenlikleri belirlenmiştir. Nem algılama özellikleri oda sıcaklığında farklı nem değerlerine göre elektriksel direncin değişimi ölçülerek tespit edilmiştir. Elde edilen filmlerin nem yakalama/bırakma kinetikleri ise QCM tekniği kullanılarak ölçülmüş ve analiz edilmiştir.

### Anahtar kelimeler

Ru katkısı; Kalay oksit;  
Sol-jel; Nem sensörü

© Afyon Kocatepe Üniversitesi

### 1. Introduction

Transparent conducting oxides have certain advantages when compared to other types of semiconductors, such as low cost, simple construction, small size and ease of placing the sensor in the operating environment. Therefore they are the popular and useful sensing materials for making inexpensive gas sensing devices (Parthibavarman *et al.* 2011). Tin (IV) oxide is a

semiconductor with a wide direct forbidden band gap of 3.6 eV and it is amenable to n-type doping. It has attracted much attention for applications involving transparent electrodes, solar cells and gas sensors since it is non toxic, inexpensive, and highly abundant (Choi *et al.* 2010; Li *et al.* 2010). Sensors in the form of thin or thick films are very attractive because they have shown distinct advantages, such as small size, simple construction, low cost and little weight (Shuping *et al.* 2008). SnO<sub>2</sub> films are

prepared by various fabrication techniques such as chemical vapor deposition (Parthibavarman *et al.* 2011), spray pyrolysis (Shuping *et al.* 2008; Choi *et al.* 2010), thermal evaporation (Li *et al.* 2010), magnetron sputtering (Liewhiran *et al.* 2009), and sol-gel method (Niranjan *et al.* 2002; Delgado 2002). Of these methods, the sol-gel process has recently attracted considerable attention inasmuch as it is proving to be an economical and energy saving method to deposit high quality films on large areas.

The present study mainly aims to investigate the Ru incorporation on the structural and optical properties of SnO<sub>2</sub> films deposited sol-gel method. To the best of our knowledge, this is the first report on physical properties of SnO<sub>2</sub> films by Ru doping.

## 2. Materials and Methods

Undoped and Ru doped SnO<sub>2</sub> films were deposited on glass substrate by sol-gel technique. Tin (II) chloride dihydrate (Aldrich) precursor was used as starting material. The dopant source of ruthenium came from ruthenium (III) chloride (Aldrich). These salts were first dissolved in methanol at room temperature. Small amounts of glacial acetic acid were added to all solutions as chelating agent to form more than one bond to a metal ion. The molar ratio of Ru/Sn were maintained 1:1. The Ru/Sn nominal volume ratio was 10 %. The obtained solution was stirred in an ultrasonic cleaner at room temperature for 2 hours in air to obtain intended homogeneity and turbidity. Glass substrates were cleaned in methanol for 2 hours in an ultrasonic cleaner prior to spin coating process. The solution was dropped onto glass substrates rotated at 1500rpm for 45 s. The deposited films were then annealed at 600 °C for 1 hour in air. Coating and heating procedures were performed by three times.

X ray diffraction (XRD, Rigaku D/MAX 2200/PC) patterns of the films were determined to identify phase structure by means of a diffractometer with a CuK $\alpha$  irradiation. The surface properties and

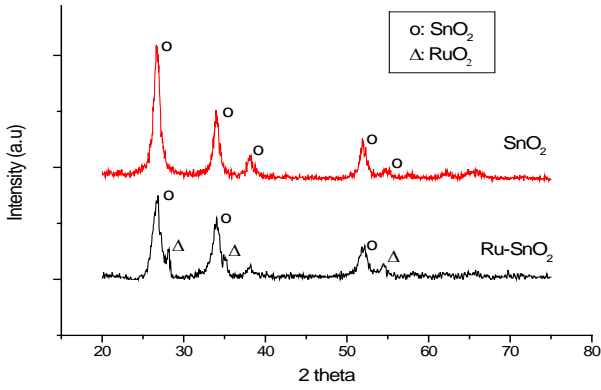
topographies of the films were examined using scanning electron microscopy (SEM, JEOL JSM 6060) attached with energy dispersive spectroscopy (EDS) and atomic force microscopy (AFM, Nanosurf Easy Scan) respectively. The film thickness was determined with VEECO profilometer. Keithley 2400 and 6517 series source meter was used for electrical measurements. QCM with the model of CHI400A Series from CH Instruments (Austin, USA) has been used to measure the change in the resonance frequency due to mass loading of water molecules after exposure of the QCM electrodes for various humidity levels.

## 3. Results and Discussions

### 3.1. Structural and morphological properties

XRD patterns of undoped and Ru doped SnO<sub>2</sub> thin films deposited on Si substrates were represented in Figure 1. Bragg peaks due to the presence of SnO<sub>2</sub> rutile phase were observed in both of the films. In Ru doped SnO<sub>2</sub> film, both SnO<sub>2</sub> and RuO<sub>2</sub> peaks were obtained. Bragg peaks for RuO<sub>2</sub> phase were found to be at smaller intensities if compared to SnO<sub>2</sub> peaks. This result also notes that substitution of Ru into tetragonal rutile structure was successfully applied.

Sol-gel deposition is a wet chemical route and the film quality is directly related to various parameters such as substrate interaction, pH, humidity and temperature. In order to produce crack-free and pinhole-free, oriented and homogenous films, optimization of these parameters and the control of experimental conditions are found to be very important. Films which will be candidates for a member of electronic sensor device must obtain all properties mentioned in the above paragraph. Intended material which will act as a gas or humidity sensor will work electronically. By this way any crack or inhomogeneity will destroy the electronic structure of the films. Figure 2 represents microstructure and morphology of the smooth and crack-free undoped and Ru doped SnO<sub>2</sub> films.



**Şekil 1.** XRD patterns of undoped and Ru doped SnO<sub>2</sub> nanostructure thin films on glass substrates.

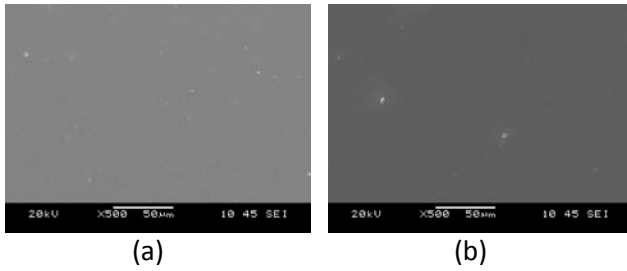


**Figure 2.** SEM images of (a) undoped and (b) Ru doped SnO<sub>2</sub> nanostructure thin film.

In order to support SEM results and determine surface roughness of the films, AFM analyses were applied. AFM results were depicted in Figures 3a and 3b for undoped and Ru doped SnO<sub>2</sub> films respectively. AFM image of the film represents nanoscale surface roughness between 1 and 20 nm. It is clear from SEM and AFM micrographs that higher part of region represent white region.

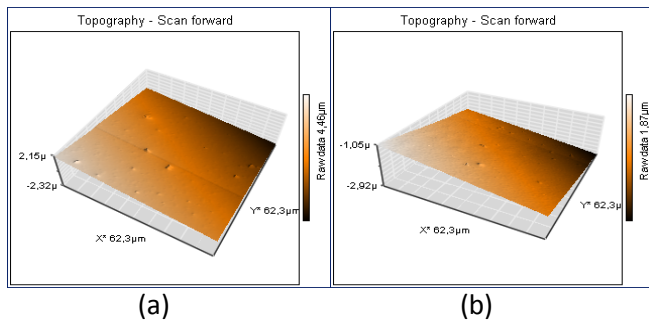


**Figure 3.** AFM images of (a) undoped and (b) Ru doped SnO<sub>2</sub> nanostructure thin film.

### 3.2. Electrical properties

The current–voltage (I–V) characteristic of the p-Si/SnO<sub>2</sub> diode is shown in Figure 4a and p-Si/Ru-doped SnO<sub>2</sub> diode is shown in Figure 4b. At low voltages, the forward current of the diode

increases exponentially with applied voltage. The device indicates a rectifying behavior between SnO<sub>2</sub>-Ru-doped SnO<sub>2</sub> and p-Si semiconductors. At low voltages, the nanostructure of p-Si/SnO<sub>2</sub>-Ru-SnO<sub>2</sub> junctions behave like a Schottky barrier diodes. The current–voltage characteristics of the p-Si/SnO<sub>2</sub>-Ru-SnO<sub>2</sub> diodes can be analyzed by the following relation (Rhoderick and Williams 1988; Cheung and Cheung 1986),

$$I = I_0 \exp\left(\frac{qV}{nkT}\right) [1 - \exp\left(-\frac{qV}{kT}\right)] \quad (1)$$

where V is the applied voltage, n is the ideality factor, k is the Boltzmann constant, T is the temperature q is the electronic charge and I<sub>0</sub> is the reverse saturation current given by,

$$I_0 = AA^* T^2 \exp\left(\frac{-(q\phi_B)}{kT}\right) \quad (2)$$

where A is the contact area, A\* is the Richardson constant (32Acm<sup>-2</sup> K<sup>-2</sup> for p-Si) and φ<sub>B</sub> is the barrier height. The barrier high of the diode was calculated using the reverse saturation current. Reverse saturation current I<sub>0</sub> values for SnO<sub>2</sub> and Ru-doped SnO<sub>2</sub> diodes were found to be 3,95x10<sup>-6</sup> eV and 3,72x10<sup>-5</sup> eV. The ideality factor of the diode was determined from the slope of the linear region of ln I– V characteristics in forward bias region of Fig. 4 and obtained n values is higher than unity were found to be 1.53 for SnO<sub>2</sub> diode, 1,99 for Ru-doped SnO<sub>2</sub> diode. The higher value of ideality factor of the p-Si/SnO<sub>2</sub>-Ru-SnO<sub>2</sub> diodes are attributed to the interface states and series resistance effects. These effects cause the non-ideal behavior.

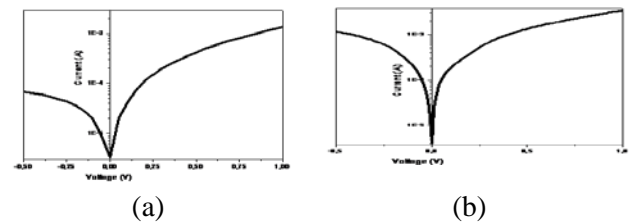


**Figure 4.** Current-voltage characteristics of the nanostructure (a) SnO<sub>2</sub>/p-Si (b) Ru-SnO<sub>2</sub>/p-Si diodes.

The effect of series resistance can be analyzed by Cheung’s method defined by the following relations (Cheung and Cheung 1986),

$$dV/(d\ln(I)) = nkT/q + IR_s \quad (3)$$

$$H(I) = V - n kT/q \ln\left(\frac{I_0}{AA^* T^2}\right) = IR_s + n\phi_B$$

(4)

The  $R_s$  is the series resistance and series resistance is an important effects on I-V characteristics of metal/semiconductor junction. These effects cause the non-ideal behavior.  $R_s$  values were calculated from intercept of  $dV/d\ln I$  vs.  $I$  plot shown in Fig. 5. (a) and (b) and  $n$  values were calculated from the slope of forward bias  $\ln I$ -V curve at room temperature shown in Figure 4. (a) and (b) was found to be 391.1 k $\Omega$  and 1.58 for SnO<sub>2</sub> diode, 289.2 k $\Omega$  and 1.91 for Ru-doped SnO<sub>2</sub> diode respectively.  $n$  value is measure of the conformity of the diode behaviour to pure thermoionic emission. The obtained ideality factor for p-Si/SnO<sub>2</sub> diode is lower than the study in literature (Caglar *et al.* 2009; Altindal *et al.* 2003; Sze 1981). This may result from the high probability of electron and hole recombination in the depletion region or occurrence of tunneling current or presence of an interfacial layer.

Figures 5a and 5b show of  $dV/d\ln I$  vs.  $I$  and  $H(I)$  vs.  $I$  plots. The plot of  $H(I)$ - $I$  will give a straight line whose slope and intercept are  $R_s$  and  $n\phi_B$ .  $n$  values are known and the  $R_s$  and  $\phi_B$  values were found to

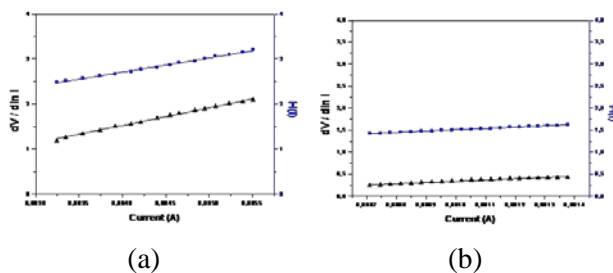


**Figure 5.** Plots of  $dV/d\ln(I)$  vs.  $I$  and  $H(I)$  vs.  $I$  of the nanostructure (a) SnO<sub>2</sub>/p-Si (b) Ru-SnO<sub>2</sub>/p-Si diodes.

be 316 k $\Omega$  and 0.83 eV for SnO<sub>2</sub> diode, 301.6 k $\Omega$  and 0.65 eV for Ru-doped SnO<sub>2</sub> diode, respectively. The  $\phi_B$  value was found 0.87 eV in literature (Caglar *et al.* 2009). The  $R_s$  and  $\phi_B$  values obtained from the Cheung's functions are in agreement with each other due to consistency of Cheung's functions. The average series resistance was obtained to be 353.5 k $\Omega$  for SnO<sub>2</sub> diode and 295.5 k $\Omega$  for Ru-doped SnO<sub>2</sub> diode. Ruthenium addition is decreased the resistance value and

makes the diode more conductive. The obtained series resistance is an important factor in performance of the diodes and affects current-voltage characteristic of the diode. The magnitude of  $R_s$  obtained causes a deviation from the linearity in the forward current region and furthermore, series resistance causes a voltage drop across the interface layer of the diode. As seen in Figures 4a and 4b after about 0.05 V and 0.04 V, the forward bias characteristics of the nanostructure SnO<sub>2</sub> and Ru-SnO<sub>2</sub>/p-Si diodes deviate from linearity. This deviation results from the series resistance. When the series resistance is low, the I-V curve yields a straight line over a longer range. The series resistance leads to a reduction of the voltage across the barrier region. The precise ideality factors of SnO<sub>2</sub> and Ru-doped SnO<sub>2</sub>/p-Si diode ( $n=1.58, 1.91$ ) and barrier heights ( $\phi_B=0.83\text{eV}, 0.65\text{eV}$ ) at the room temperature are larger than that of the conventional Al/p-Si Schottky diode ( $n=1.02$ ) and ( $\phi_B=0.58\text{ eV}$  ). This indicates that SnO<sub>2</sub> and Ru-doped SnO<sub>2</sub> interfacial layers modify the barrier high of the diode by forming of a physical barrier between the metal and the Si wafer. Addition of ruthenium is increased the ideality factor ( $n$ ) and reverse saturation current ( $I_0$ ) but the value of barrier height and series resistance is decreased. This suggests that addition of ruthenium modifies the barrier height due to the shift in the work function of the metal and in the electron affinity of the semiconductor.

### 3.3. Humidity sensor properties

Figure 6 shows measured resistance changes of undoped and Ru- doped SnO<sub>2</sub> films. The relative humidity (RH) lies in the range of 20% and 70%. RH values is presented on the right side of the plot, while corresponding resistance of these films are given on the left side of the plot. Resistance of the bothe films are changed on the order of 3 under the voltage as a result of the possible disassociation of the adsorbed moist molecules on the oxygen vacancies on the SnO<sub>2</sub> surface.

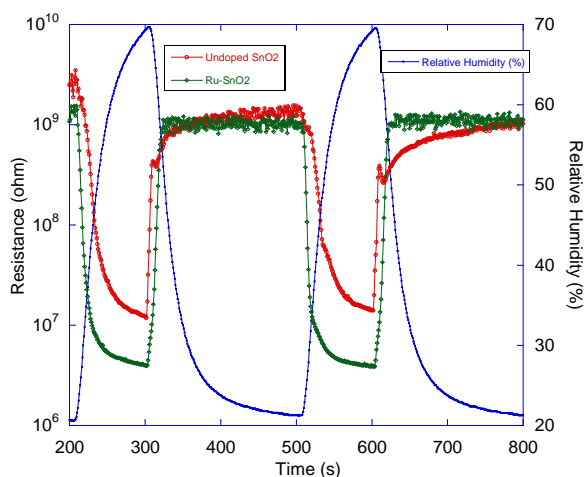


**Figure 6.** Resistance response undoped and Ru doped  $\text{SnO}_2$  films under different humidity levels.

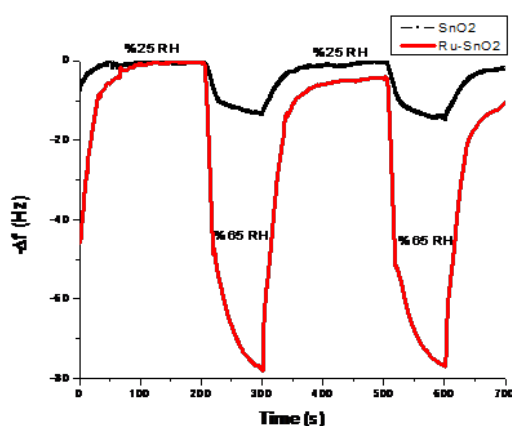


**Figure 7.** QCM response undoped and Ru doped  $\text{SnO}_2$  films under different humidity levels.

Figure 7 shows adsorptions-desorptions responses of both films when sent only dry and wet air consequently with 200s/100s periods to observe maximum adsorption and desorption kinetics. The results show that the response time against quick relative humidity changes of these sensors are less than 25 s for adsorption process, while it is around 50 s, that is, 2 times larger for desorption processes.

#### 4. Conclusions

Undoped and Ru doped nanostructure  $\text{SnO}_2$  films were deposited on both glass and Si substrates by sol-gel technique. Structural, electrical and sensor properties were significantly altered with Ru doping into  $\text{SnO}_2$  films. XRD results revealed that all the films have tetragonal rutile and Ru incorporation affects the crystalline structure of the film. It was observed that surface was

smoother with adding Ru. The current–voltage characteristics of both undoped and ru-doped  $\text{SnO}_2$  show non-ideal contact behaviour with the ideality factor higher than unity. The resistance of these sensors decrease by about 3 orders of magnitude with increasing relative humidity (RH) from 20% to 70% RH. The response and recovery time of the sensor are around 25 s and 50 s, respectively. Thus, QCM results show that these films are very sensitive to relative humidity changes and give reproducible adsorption and desorption kinetic behaviors for both short and long time periods and can be used for potential humidity sensor applications.

#### Acknowledgement

This project was partially supported by Ege University and Dokuz Eylul University Scientific Research Projects. The authors thanks to Dr. Salih Okur, Orkut Sancakoğlu and Fevzi Sümer for their characterization and humidity measurements.

#### References

- Altindal, S., Karadeniz, S., Tugluoğlu N., and Tataroglu, A., 2003, *Solid State Electron.*, **47**, 1847.
- Caglar, Y., Caglar, M.S., Ilcan, Yakuphanoglu, F., 2009, *Microelectronic Engineering*, **86**, 2072- 2077.
- Cheung, S.K., Cheung, N.W., 1986, *Appl. Phys. Lett.* **49** 85.
- Choi Y. J., Park H., Gollledge S., Johnson D., Chang H.J., Jeon H., 2010. *Surface & Coatings Technology*, **205** (2010) 2649–2653.
- Delgado R.D., 2002, Tin Oxide Gas Sensors: An Electrochemical Approach.
- Li L., Yu K., Wu J., Wang Y., & Zhu, 2010. *Cryst. Res. Technol.* **45**, No. 5, 539 – 544 (2010)/DOI 10.1002/crat.200900718.
- Liewhiran C., Tamaekong N., Wisitsoraat A., & Phanichphant S., 2009, *Sensors*, **9**, 8996 9010.
- Niranjan R. S., Sainkar S.R., Vijayamohan K., Mulla I.S., 2002, *Sensors and Actuators B*, **82**, 82-88.
- Parthibavarman M., Hariharan V. and Sekar C., 2011. *Materials Science and Engineering*.
- Rhoderick, E.H., Williams, R.H., Metal Semiconductor Contacts, Clarendon, Oxford, 1988.
- Shuping G., Jing X., Jianqiao L., Dongxiang Z., 2008. *Sensors and Actuators B*, **134**, 57–61.
- Sze, S.M., Physics of Semiconductor Devices, (Ed.), John Wiley & Sons, New York, 1981.